EPITHERMAL NEUTRON SOURCE BASED ON ^{7}Li(p,n)^{7}Be REACTION OPTIMIZATION FOR NEUTRON CAPTURE THERAPY.

O. Kononov, V. Kononov, V. Korobeynikov, N. Soloviev, M. Bokhovko, D. Sanin, W. Chu, A. Zhitnik, S. Ognev

ABSTRACT

In report presented investigations of patient treatment possibility by boron neutron capture therapy (BNCT) on special facility created in Institute for Physics and Power Engineering (IPPE) based on high current proton accelerator KG-2,5 with a ^{7}Li(p,n)^{7}Be reaction as neutron source. Detail data on yield and spatial-energy distribution of neutrons from this reaction with calculated absorbed dose distribution in patient tissue are presented for two modifications of a neutron source: near threshold with natural neutron beam kinematical collimation and with proton energy considerably high then reaction threshold with using beam shaping assembly for neutron moderation and epithermal beam forming.

1. INTRODUCTION

Nowadays neutron capture therapy looks very promising method of cancer treatment, especially for brain tumors by reason of selective damage cancer cells. Treatment effect of this method based on neutrons nuclear reaction with nuclides ^{10}B, ^{157}Gd. These nuclides have high cross-section of interaction with thermal neutrons. Unfortunately, thermal neutrons could enter only in near surface tissue and could not be used for deep localized tumors. This restriction makes possible to use such neutrons only for surface tumors or for intraoperative therapy. For deep situated tumors looks more prospective to use epithermal neutrons with energy from 1 eV to 10 keV. These neutrons have much more penetrative ability and slow down in tissue till thermal energy. It makes possible neutron capture therapy for tumors located on depth up to 10 cm from surface. Important, that in epithermal neutron beam fast neutrons number must be as small as possible, because of dose from high-energy neutrons is main factor limited treatment process. Main critical factor is surface absorbed dose form reaction with fast neutrons. For treatment purposes necessary to have epithermal neutrons beam with size about 10x10 cm and neutron flux $\sim 10^9$ s^{-1} cm^{-2}.

Now on nuclear reactors was created some facilities [1-4] with complex moderator system, filters, collimators and shielding for epithermal neutron beam creation. Epithermal neutron beam with better for neutron capture therapy characteristics (FCB MIT) was created on 5MW nuclear reactor MITR-II in USA [3, 4]. On this facility thermal neutron beam converted by ^{235}U in to fission spectra neutron beam which then transformed in to epithermal beam. Although nuclear reactor as an intensive neutron source has such important for neutron therapy feature as high stability of neutron current, construction such facility series in big oncology clinics

looks not possible, because of necessary to satisfy special nuclear safety requirements, high expenses for building and maintain.

Thereby in last ten years are wide discussed and investigated idea to create neutron source for neutron capture therapy based on low cost proton accelerator with energy 2-3 MeV and beam power 10-20 kW [5-8] to be installed directly in hospital. Presently ^{7}Li(p,n)^{7}Be reaction looks are most appropriate neutron source for accelerator based facility for neutron capture therapy [9]. Total neutron yield from thick (in comparison with proton stopping depth) metallic lithium-7 target with starting proton energy 2.5 MeV and beam current 10 mA is about 10^{13} neutrons per second and neutrons energy are less then 0.78 MeV. Previous calculations [5-7] are shown that with such neutron source by using compact moderator it is possible to create good for neutron capture therapy neutron beam. Main goal of this investigations are based on calculations to find what materials are better to use in moderator and to optimized moderator size and then obtain epithermal neutron beam characteristics after moderation.

2. MATERIALS AND METHODS

2.1 Neutron source modeling

Spatial-energy distribution of ^{7}Li (p,n) ^{7}Be neutrons from thick ^{7}Li metal target for various incident energies protons was calculated with using of techniques and programs described [10]. For detail representation of neutrons spatial distribution, the subinterval 1º along the angle of neutrons flight escape to direction of protons beam was used. As an example on fig.1 the neutrons energy distributions from thick ^{7}Li target for angles 0º, 45º and 90º for incident protons energy 2.3 MeV are represented. The angular neutrons yield distribution from thick target in a laboratory system for the same protons energy is represented on fig. 2. The full calculated yield of neutrons under initial energy of protons 2.2 MeV, 2.3 MeV, 2.4 MeV, 2.8 MeV, for which the basic investigations were carried out, are $3.9\cdot10^{12}$, $6.3\cdot10^{12}$, $8.1\cdot10^{12}$ and $1.37\cdot10^{13}$ neutrons per second for the beam current 10 mA. These dates are in a good agreement with direct neutrons full yield measurements [6, 11].

In parallel with neutrons in lithium target gamma rays are born, which basic source are ^{7}Li$(p, p'\gamma)$^{7}Li reaction and radionuclide ^{7}Be. Gamma rays yield with energy 0.478 MeV from ^{7}Li$(p, p'\gamma)$^{7}Li reaction, calculated for thick ^{7}Li target by a method and programs, described [10], for the same protons energy are $2.3\cdot10^{12}$, $2.8\cdot10^{12}$, $3.2\cdot10^{12}$, $5.1\cdot10^{12}$ gamma quantum per second for beam current 10 mA. Its angular distribution is close to isotropic. These dates are in a good agreement with direct gamma rays yield from ^{7}Li$(p, p'\gamma)$^{7}Li reaction measurements [12].

During target irradiation by protons accumulation of radioactive nuclide ^{7}Be, had a half-life 53.3 days, occurs. The decay of ^{7}Be in 89.7 % of cases is electron capture in a basic state, which is not accompanying with an emission of hard radiation, and in 10.3 % of cases - in the first excited state ^{7}Li with a consequent emission of gamma quantum with energy 0.478 MeV. As a result, after 1 hour irradia-

tion of thick ^{7}Li target by protons with energy 2.5 MeV and beam current 10 mA, the target will be a source of gamma rays with energy 0.478 MeV and activity $5.4 \cdot 10^8$ Bk.

2.2 Simulation of radiation transport

Neutrons and gamma rays transport simulation was carried out by Monte Carlo method using programs C-95 and MCNP [13, 14]. To investigate various materials properties as a moderator for creation of epithermal neutrons beam sphere moderator model was used. In its center was placed neutron source as a thin disk with diameter 4 cm to which the cylindrical cavity with the same diameter (fig.3) adjoins. Detectors were ring surfaces of sphere taken with subinterval 30º relative to directions of protons beam and having an opening angle ±15º. Energy groups, into which the neutrons and gamma quantum were divided, are presented in tab.1 and 2. Calculations were carried out for sphere radius from 16 to 28 cm.

As a criterion for the choice of material and optimal size of moderator two parameters were choused: ϕ_{epi} - epithermal neutrons flux density (neutrons energy more 1 eV) on a moderator surface for proton beam current 10 mA, and $\dot{D}/\phi_{epi}$ - magnitude biologically weighed absorbed dose specific power created in the same point in tissue by neutrons and a gamma quantum, reduced to a single epithermal neutrons flux density on a moderator surface. The kerma-factors values and relative biological effectiveness presented in tab. 2, were used for calculation of biologically weighted doses. The magnitude $\dot{D}/\phi_{epi}$ is equivalent relative biological effectiveness weighed kerma-factor for a tissue and it is desirable, that it did not exceed magnitude biologically weighed dose specific power arising under epithermal neutron transport in phantom which is $\sim 2.8 \cdot 10^{-12}$ RBE Gy cm^2. These two parameters are usually neutron beam in air dosimetric qualities parameter. Calculations results in these coordinates (fig.5-8) visually illustrate the quality of moderator: the best result corresponds to the left top of the graph.

More detail information about epithermal neutrons beam characteristics was obtained in absorbed dose distribution in the phantom calculations. In these calculations special moderator block configuration was used fig.4. It allows to simulate moderator block composed from different materials, and also to take into account real construction of the moderator block, including accelerator target. In these calculations same simplified model of the phantom was used (cube with rib 20 cm). The first two cube layers with thickness 0.5 and 0.8 cm simulate skin and skull accordingly, and rest of volume - substance of brain. The structure of tissue corresponds to the recommendations ICRU-46 [15]. Ring detectors with radius subinterval 1 cm are placed on the depth of phantom in its fore-part with subinterval 1 mm in the first two layers up to the depth 1.5 cm and with subinterval 0.5 cm on the greater depth in the phantom.

2.3 Moderator choice

Calculation researches of materials that can be used as moderator or filter for forming an epithermal neutrons beam were carried out in a series of works [3-7]. Light elements materials with large fast neutrons scattering cross-section and small absorption cross-section and activation in the slow neutron range are the most preferable. Those materials are deuterium, oxides and fluorides of beryllium, magnesium, aluminum, graphite, composition of fluorine with carbon and other. Materials, contained a fluorine, which has at energy higher than 150 keV large neutron inelastic scattering cross-section with excitation of low levels with energy 0.11 and 0.197 MeV [16], are the most interest. When choosing moderator material and it optimum size for a accelerator based $^7Li(p,n)^7Be$ reaction epithermal neutrons source, source size, energy distribution and spatial anisotropy has essential meaning. The last two factors influence also on a choice of optimum positioning of irradiated object to direction of protons beam.

In performed calculations we investigated the following chemical elements and isotopes: D, ^7Li, Be, C, N, O, F, Mg, Al, Ti, Ca in available chemical combination, such as D_2O, LiF, MgF_2 , CaF_2 , polytetrafluoroethylene $(CF_2)n$, C_6F_6, AlN, Fluental®. The last material represents a metallo-ceramiks with composition: 56% F, 43% Al, 1% LiF and was specially developed for the similar purposes [17] and used to epithermal neutron beam forming in some reactors and accelerators [17, 18].

3. RESULTS

3.1. In-air neutron beam characteristics

For various materials properties evaluation from point of view optimum epithermal neutron beam forming, using $^7Li(p, n)^7Be$ reaction, calculations for moderator model as sphere (fig.3) with radiuses 16, 18, 20, 22, 24, 26 and 28 cm were carried out. Main calculations have performed for a neutrons source with starting protons energies 2.3 MeV and beam current 10 mA. Statistical error of calculations was less than 1%. Calculations epithermal neutrons flux density comparison and parameter $\dot{D}/\phi_{epi}$ on a surface for one of investigated moderator with various radius R values, obtained by Monte Carlo codes C-95 and MCNP and presented in a table 1, shows their satisfactory consent in limits of statistical error. Calculations results for various materials are represented in fig. 5 - 8. From figures one can be seen that epithermal neutrons flux density on a moderator surface for most materials is similar on magnitude and as a first approximation corresponds to dependence $1/R^2$, that follows from small neutrons absorption in moderator. Deuterium and beryllium possessing by large stopping ability ($\xi\Sigma_s$ for a deuterium and beryllium ~ 0.15 cm^{-1} up to neutrons energy ~ 100 keV), are elimination, therefore already for moderator thickness 16 cm the significant part of neutrons are slowing up to energies below than accepted epithermal area boundary 1 eV. As a result the epithermal neutrons

flux density for deuterium and beryllium moderator radius 16 cm appears 1.2-1.5 times smaller and corresponds to dependence $\sim 1/R^4$. Second feature of moderator from deuterium and beryllium, and also graphite, which have a smooth dependence of total cross-section from neutrons energy, is the considerable difference epithermal neutrons beam characteristics leaving moderator under angles 0º and 90º in relation to direction of proton beam (collinear and orthogonal geometry). Orthogonal geometry, as one can see from fig. 5, for deuterium has some advantages, providing forming epithermal neutron beam with lower fast neutrons impurity and flux density ~1.2 times greater. The similar result is observed for beryllium and carbon. For moderators including isotopes with resonance structure in total neutron cross-section (fluorine, magnesium, aluminum) difference between orthogonal and collinear geometries is insignificant. Results presented on fig. 6-8 are for collinear geometry.

Second parameter defined epithermal neutron beam quality is value of the equivalent kerma-factor $\dot{D}/\phi_{epi}$ averaged on a neutron spectrum. Mainly it value is determined by protons recoil, and directly connected with fast neutrons number in spectrum and 20-30 times for researched materials. The kerma-factor $\dot{D}_\gamma/\phi_{epi}$, connected with gamma rays from accompanying reactions in the target and gamma rays born in moderator, for investigated materials does not exceed 10% from $\dot{D}/\phi_{epi}$. From figures 6-8 could be ssen, that the best characteristics have epithermal neutrons beams formed by moderators from MgF_2, BeF_2 and polytetrafluoroethylene. The most perspective materials are magnesium fluoride (density 3.14 g/cm^3) and polytetrafluoroethylene (density 2.1 g/cm^3). Both these materials are commercially available and have high purity. Beryllium fluoride moderator not looks prospective because of high beryllium toxicity. As could be seen from the fig. 5, 6, 8, using the ^7Li (p,n) ^7Be reactions for proton energy 2.3 MeV as a neutron source, Fluental® is less suitable moderator in a comparison with MgF_2 and polytetrafluoroethylene.

Results of comparison LiF_2 properties with various content of ^6Li were compared with MgF_2 and polytetrafluoroethylene are given on the Fig. 7. Taking into account the high price of LiF_2, depleted with isotope ^6Li this material as a moderator looks not perspective.

So, the most perspective moderators for epithermal neutron source based on $^7Li(p,n)^7Be$ reaction are MgF_2 and polytetrafluoroethylene. These moderator materials are formed epithermal neutrons spectrum, which give the most accordance with BNCT demands. The comparison of neutron spectrum from sphere with radius 20 cm from MgF_2, polytetrafluoroethylene, Fluental® and carbon moderators are given on Fig. 9, 10. Clear that MgF_2 and polytetrafluoroethylene give the smallest part of fast neutron and have the sharp peak in distribution region 1-20 keV.

Polytetrafluoroethylene technology admits to insert to its composition without any complications different additions, for example, a powder MgF_2 or PbF_2. The first one is interesting with point of view of improving polytetrafluoroethylene characteristics as a moderator and second one with point of view absorption

gamma ray. MgF$_2$ and polytetrafluoroethylene comparison properties with combined composition and Fluental® is given on Fig. 8.

At the same time elastic and inelastic scattering, radiative capture are occurred when neutron transport in moderator of MgF$_2$ and polytetrafluoroethylene. As a result of capture the radioactive nuclides ^{20}F with T$_{1/2}$ = 11.4 sec. and ^{27}Mg with T$_{1/2}$ = 10 min are generated. Their decay accompanying with emission 0.8-1.6 MeV gamma ray. Calculation of ^{20}F and ^{27}Mg production rate in MgF$_2$ and polytetrafluoroethylene moderators with radius 20 cm showed that total activities in full moderator volume for protons starting energy 2.3 Mev and current 10mA are $3,8 \cdot 10^{10}$ Bq and $6,7 \cdot 10^8$ Bq accordingly and corresponding kerma factor $\dot{D}_{\gamma\,act}/\phi_{epi}$ is not exceed 1% from $\dot{D}/\phi_{epi}$ value.

During epithermal neutron source optimization arisen problem proton beam energy choice. With proton energy increasing total neutron yield from thick target is increased too. At the same time primary neutron energy is increased, so moderator size must be increased. When protons energy increasing thermal power in target is increased too and additional technical difficulties will be appear. To estimate these effects calculations for different proton energy were made. Calculation results for MgF$_2$ moderator are given on Fig. 11. These results are shown that suitable energy value is in interval 2,3 – 2,8 Mev.

The comparison of epithermal source characteristics based on ^{7}Li $(p,n)^7$Be reaction with MgF$_2$ and polytetrafluoroethylene moderators (E$_p$ = 2,3 МэВ, I$_p$ = 10 мА), near threshold source (E$_p$ = 1,915 МэВ, I$_p$ = 10 мА) [19], and sources on the base of nuclear reactors [20] are given on the Fig. 12. It can be see that parameters of epithermal neutron accelerator based beams and most existing reactors are comparable as well epithermal fluxes density value as equivalent kerma factors ones.

3.2. In-phantom dose distributions

Main epithermal neutron beam characteristic from BNCT point of view is in-phantom biological weighted doses. For providing these studies moderator block configuration given on Fig.4 and phantom described in 2.2 section were used. The main calculations were done for moderator blocks with size 40x40x40 cm for initial proton energy 2.3 Mev. Biologically weighted dose distributions on the phantoms depth for three moderators materials are given on Fig. 13-15. In dose calculations were assumed that ^{10}B concentration in health tissue is 18 ppm, in tumor tissue is 65 ppm, ^{10}B$(n,\alpha)^7$Li reaction CBE products – 1.3 and 3.8 [20, 21]. Kerma-factors and RBE for neutron are given in Table 1.

The quality of epithermal neutron beam is usually characterized by next principal parameters:

1. Advantage depth (AD) – depth on which the biologically weighted dose in tumor equal with maximum dose in healthy tissue.

2. Advantage depth dose rate (ADDR), which characterizes time for achievement dose on the depth AD.

3. Therapeutic ratio (TR) dose in tumor to maximum dose in healthy tissue.

4. Advantage rate (AR) - full dose in tumor tissue to full dose in healthy tissue, integrated from surface to depth AD.

5. Current to flux ratio, J_{epi}/ϕ_{epi}, characterizing the diverge of epithermal neutron beam.

Calculated therapeutic ratio for moderators from MgF_2, polytetrafluoroethylene, Fluental® and dosimetrical measurements therapeutic ratio for FCB MIT epithermal beam [21] are given on Fig. 16.

Comparison shown that MgF_2 moderator has the best characteristics close to ones obtained on the reactor beam FCB MIT. Polytetrafluoroethylene, as a moderator, worse than MgF_2 on its characteristics but significant better than Fluental®. Because polytetrafluoroethylene is more cheaper than MgF_2, calculations were made for combined moderator, which central part is presented as a 20x20 cm^2 cross-section MgF_2 parallelepiped, remaining part consisted of polytetrafluoroethylene. Moderator thickness was varied in limit from 16 to 24 cm. Obtained results are given on Fig. 17 and shown that the optimal moderator length of MgF_2 equals approximately 20-22 см. Principal combined moderator characteristics from MgF_2 and polytetrafluoroethylene with size 40x40 cm and optimal length are given in Table 4. For comparison characteristics of FCB MIT beam [21] are given in Table 4 too. On fig. 18 given the principal parameters comparison for combined moderator from MgF_2 and polytetrafluoroethylene with calculation results for moderator, which will be used on Birmingham University facility. This moderator consist of Fluental® and carbon [18]. It is shown that proposed combined moderator has preference by all parameters as compare proposed to use in Birmingham.

CONCLUSION

Calculation studies on moderator material chouse for epitermal neutron beam creation for boron neutron capture therapy based on protons accelerator and $^7Li(p,n)^7Be$ as a neutron source are performed. Shown, that best moderator material is MgF_2. Suggested optimized moderator configuration from polytetrafluoroethylene and MgF_2. As calculation results shown that with using such moderator and proton beam with energy 2.3 MeV and current 10 mA Advanced Depth (AD) is 9 cm, Therapeutic Ratio (TR) on phantom depth 3 cm is 6, Advanced Depth Dose Rate (ADDR) on phantom depth 9 cm is ~1 Gy-equivalent per minute which equal maximum therapy time 12 minute.

REFERENCES

1. R.L. Moss, D. Beynon et al. "The requirements and development of neutron beams for neutron capture therapy of brain cancer". J. Neuro-Oncology v. 33, 27-40, 1997.
2. J. Burian, M. Marek et al. "The BNCT facility at the Nuclear Research Institute (NRI) reactor in the Czech Republic". Advance in Neutron Capture Therapy. v. 1, Medicine and Physics, 391-395. Ed. by B. Larsson et al. Elsevier Science, 1997.
3. W.S. Kiger III, S. Sakamoto, O.K. Harling "Neutronic design of a fission converter-based epithermal neutron beam for neutron capture therapy". Nucl. Sci. Eng. v. 131, 1-22, 1999.
4. O.K. Harling, K.J. Railey et al. "The fission converter-based epithermal neutron irradiation facility at the Massachusetts institute of technology reactor". Nucl. Sci. Eng. v. 140, 223-240, 2002.
5. C.-K. Chris Wang, T.E. Blue, R. Gahbauer. "A neutronic study of an accelerator-based neutron irradiation facility for boron neutron capture therapy". Nucl. Tech. v. 84, 93-107, 1989.
6. D.A. Allen, T.D. Beynon. "A design study for an accelerator based epithermal neutron beam for BNCT". Phys. Med. Biol. v. 40, 807-821, 1995.
7. D.L. Bluel, R.J. Donahue et al "Designing accelerator-based epithermal neutron beams for boron neutron capture therapy". Med. Phys. v. 25, 1725-1734, 1998.
8. B.F. Bayanov, M.V. Bokhovko, V.N. Kononov et al. "Accelerator-based neutron source for the neutron capture and fast neutron therapy at hospital. Nucl. Inst. and Meth. in Phys. Res. A413, 397-426, 1998.
9. V.N. Kononov, Yu. Ya. Stavisski. "Proton accelerator based neutron source for BNCT". Proc. 2nd All-Union symp. on using charged particle accelerators in national economy. Leningrad, USSR, 1-3 Oct. 1975, v. 2, 60-67, 1976 (in Russian).
10. O.E. Kononov, V.N. Kononov et al. "Accelerator based neutron sources for neutron and neutron capture therapy" Preprint IPPE-2985, Obninsk, 2003.
11. M. Scott. "The rate of energy loss and neutron yield for protons on thick lithium targets at energies from 3-10 MeV". Jorn. of Nucl. En., v.25, 405-416, 1971.
12. V.N. Kononov et al. "Gamma rays radiation of ^{7}Li(p,n)^{7}Be reaction based neutron source". Preprint IPPE-2643, Obninsk, 1997.
13. A.K. Zhitnik, "Monte Carlo method in VNIIEF". Questions of atomic science and technology. Series: Physical process mathematical modeling. Issue 2, 61-64, 1993.
14. J. Briesmeister "MCNP – A general Monte Carlo n-particle transportation code". LA-1625-M, version 4B, LANL, 1997.

15. J. Goorley, W.S. Kiger III, R.G. Zamenhof. "Reference dosimetry calc. for NCT with comparison of analytical and voxel models", Med. Phys. v. 29, 145-156, 2002.

16. A.I. Lashuk, I.P. Sadohin. "Gamma rays generation cross-sections in non-elastic neutrons reaction". Questions of atomic science and technology. Series: Nuclear constants, issue. 1, 26-78, 1994.

17. I. Auterinen and P. Hiismaki, "Epithermal BNCT neutron beam design for a TRIGA II reactor". Advance in Neutron Capture Therapy. Plenum press, NY, 1993.

18. T.D. Beynon, K.S. Forcey et al. "Status of the Birmingham accelerator-based BNCT facility". Research and development in neutron capture therapy, 225-228. Monduzzi Editore, 2002.

19. O.E. Kononov, V.N. Kononov, W.T. Chu, N.A. Soloviev. "Investigations of near threshold ^{7}Li(p,n)^{7}Be neutron source for neutron capture therapy". Preprint IPPE-2951, Obninsk, 2002; Atomnaja Energia, v. 94, 469-472, 2003.

20. O.K. Harling, K.J. Riley. "A critical assessment of NCT beams from fission reactors". Research and development in neutron capture therapy, 159-162. Monduzzi Editore, 2002.

21. P.J. Binns, K.J. Riley, O.K. Harling. "Dosimetric comparison of six epithermal neutron beams using an ellipsoidal water phantom". Research and development in neutron capture therapy, 405-409. Monduzzi Editore, 2002.

Table 1
Neutron Kerma-factors, RBE and CBE for basic tissue components.

Neutron energy	MeV	Hydrogen Proton recoil kerma-factors	RBE	Boron-10 Kerma-factors	CBE	Nitrogen Kerma-factors	RBE	Oxigen Kerma-factors	RBE
From	To	cGy cm^2		cGy cm^2	healthy/ tumor tissue	cGy cm^2		cGy cm^2	
0	2,15E-07	6,10E-15	1,0	7,70E-06	1,3/3,8	7,08E-10	3,2	3,73E-17	3,2
2,15E-07	4,65E-07	3,30E-14	1,2	2,47E-06	1,3/3,8	2,27E-10	3,2	9,28E-17	3,2
4,65E-07	1,00E-06	6,97E-14	1,2	1,68E-06	1,3/3,8	1,55E-10	3,2	1,88E-16	3,2
1,00E-06	2,15E-06	1,48E-13	1,2	1,15E-06	1,3/3,8	1,05E-10	3,2	3,97E-16	3,2
2,15E-06	4,65E-06	3,19E-13	1,2	7,80E-07	1,3/3,8	7,19E-11	3,2	8,51E-16	3,2
4,65E-06	1,00E-05	6,86E-13	1,2	5,31E-07	1,3/3,8	4,90E-11	3,2	1,83E-15	3,2
1,00E-05	2,15E-05	1,47E-12	1,2	3,62E-07	1,3/3,8	3,34E-11	3,2	3,94E-15	3,2
2,15E-05	4,65E-05	3,18E-12	1,2	2,47E-07	1,3/3,8	2,28E-11	3,2	8,49E-15	3,2
4,65E-05	1,00E-04	6,85E-12	1,2	1,68E-07	1,3/3,8	1,56E-11	3,2	1,83E-14	3,2
1,00E-04	2,15E-04	1,47E-11	1,3	1,14E-07	1,3/3,8	1,08E-11	3,2	3,93E-14	3,2
2,15E-04	4,65E-04	3,16E-11	1,3	7,76E-08	1,3/3,8	7,65E-12	3,2	8,49E-14	3,2
4,65E-04	1,00E-03	6,81E-11	1,4	5,27E-08	1,3/3,8	5,67E-12	3,2	1,83E-13	3,2
1,00E-03	2,15E-03	1,45E-10	1,4	3,58E-08	1,3/3,8	4,69E-12	3,2	3,93E-13	3,2
2,15E-03	4,65E-03	3,10E-10	1,5	2,42E-08	1,3/3,8	4,83E-12	3,2	8,48E-13	3,2
4,65E-03	1,00E-02	6,52E-10	1,8	1,64E-08	1,3/3,8	6,49E-12	3,2	1,83E-12	3,2
1,00E-02	2,00E-02	1,28E-09	2,0	1,14E-08	1,3/3,8	1,01E-11	3,2	3,76E-12	3,2
2,00E-02	3,00E-02	2,08E-09	2,5	8,63E-09	1,3/3,8	1,46E-11	3,2	6,43E-12	3,2
3,00E-02	4,00E-02	2,78E-09	3,0	7,32E-09	1,3/3,8	1,82E-11	3,2	9,02E-12	3,2
4,00E-02	5,00E-02	3,41E-09	3,5	6,52E-09	1,3/3,8	2,16E-11	3,2	1,16E-11	3,2
5,00E-02	6,00E-02	3,99E-09	3,6	5,96E-09	1,3/3,8	2,47E-11	3,2	1,42E-11	3,2
6,00E-02	7,00E-02	4,51E-09	3,8	5,57E-09	1,3/3,8	2,77E-11	3,2	1,67E-11	3,2
7,00E-02	8,00E-02	4,99E-09	4,2	5,26E-09	1,3/3,8	3,07E-11	3,2	1,93E-11	3,2
8,00E-02	9,00E-02	5,47E-09	4,3	5,03E-09	1,3/3,8	3,34E-11	3,2	2,18E-11	3,2
9,00E-02	1,00E-01	5,87E-09	4,4	4,82E-09	1,3/3,8	3,58E-11	3,2	2,43E-11	3,2
1,00E-01	1,50E-01	6,94E-09	4,5	4,42E-09	1,3/3,8	4,24E-11	3,2	3,15E-11	3,2
1,50E-01	2,00E-01	8,53E-09	4,5	3,89E-09	1,3/3,8	5,29E-11	3,2	4,44E-11	3,2
2,00E-01	3,00E-01	1,04E-08	4,5	3,43E-09	1,3/3,8	6,24E-11	3,2	5,82E-11	3,2
3,00E-01	4,00E-01	1,23E-08	4,5	3,03E-09	1,3/3,8	7,04E-11	3,2	7,39E-11	3,2
4,00E-01	5,00E-01	1,39E-08	4,5	2,65E-09	1,3/3,8	8,15E-11	3,2	1,21E-10	3,2
5,00E-01	6,00E-01	1,54E-08	4,4	2,57E-09	1,3/3,8	1,22E-10	3,2	2,21E-10	3,2
6,00E-01	7,00E-01	1,66E-08	4,3	2,24E-09	1,3/3,8	9,62E-11	3,2	9,05E-11	3,2
7,00E-01	8,00E-01	1,78E-08	4,2	1,71E-09	1,3/3,8	2,05E-10	3,2	1,06E-10	3,2
8,00E-01	9,00E-01	1,94E-08	4,1	1,41E-09	1,3/3,8	1,41E-10	3,2	1,25E-10	3,2
9,00E-01	1,00E+00	2,00E-08	4,0	1,20E-09	1,3/3,8	1,15E-10	3,2	2,46E-10	3,2
1,00E+00	1,50E+00	2,25E-08	3,5	1,23E-09	1,3/3,8	2,65E-10	3,2	2,71E-10	3,2
1,50E+00	2,00E+00	2,63E-08	3,2	2,39E-09	1,3/3,8	3,29E-10	3,2	2,21E-10	3,2
2,00E+00	2,50E+00	2,93E-08	2,9	2,23E-09	1,3/3,8	4,04E-10	3,2	1,43E-10	3,2
2,50E+00	3,00E+00	3,18E-08	2,7	2,73E-09	1,3/3,8	6,66E-10	3,2	1,82E-10	3,2
3,00E+00	4,00E+00	3,47E-08	2,5	2,82E-09	1,3/3,8	1,24E-09	3,2	4,61E-10	3,2
4,00E+00	5,00E+00	3,78E-08	2,2	3,13E-09	1,3/3,8	1,54E-09	3,2	4,45E-10	3,2
5,00E+00	6,00E+00	4,01E-08	2,1	2,95E-09	1,3/3,8	1,10E-09	3,2	5,00E-10	3,2
6,00E+00	8,00E+00	4,23E-08	1,9	2,53E-09	1,3/3,8	1,16E-09	3,2	7,35E-10	3,2
8,00E+00	1,00E+01	4,45E-08	1,6	3,61E-09	1,3/3,8	1,24E-09	3,2	1,00E-09	3,2

Table 2
Photon kerma-factors.

Photon energy	MeV	Kerma-factors
From	to	cGy cm^2
0,000	0,010	1,00E-08
0,010	0,015	4,80E-10
0,015	0,025	1,80E-10
0,025	0,030	9,00E-11
0,030	0,040	6,25E-11
0,040	0,050	4,09E-11
0,050	0,060	3,34E-11
0,060	0,080	3,20E-11
0,080	0,100	3,74E-11
0,100	0,150	5,36E-11
0,150	0,200	8,05E-11
0,200	0,300	1,24E-10
0,300	0,400	1,81E-10
0,400	0,500	2,36E-10
0,500	0,600	2,89E-10
0,600	0,800	3,62E-10
0,800	1,000	4,54E-10
1,000	1,500	5,86E-10
1,500	2,000	7,55E-10
2,000	3,000	9,60E-10
3,000	4,000	1,20E-09
4,000	5,000	1,42E-09
5,000	6,000	1,62E-09
6,000	8,000	1,92E-09

Table 3
Calculation results comparisons for Monte Carlo codes C-95/MCNP.

Moderator radius	16	18	20	22	24	26
Difference in epithermal flux $\phi_{y\ddot{i}e}$	1,02	1,02	1,02	1,01	1	0,989
Difference in kerma-factors $\dot{D}/\phi_{y\ddot{i}e}$	0,997	1	1	0,994	0,986	0,983

Table 4
Basic characteristics comparison of accelerator based facility with beam shaping assembly made from MgF$_2$ and polytetrafluoroethylene and FCB MIT [3, 21] facility.

	AD, cm	TR$_{max}$	ADDR, RBE cGy/min	AR	J_{epi}/ϕ_{epi}
Accelerator facility with BSA	9,1	6,2	100 (current 10 mA)	5,6	0,64
FCB MIT	9,3	6,4	125	6	0,65
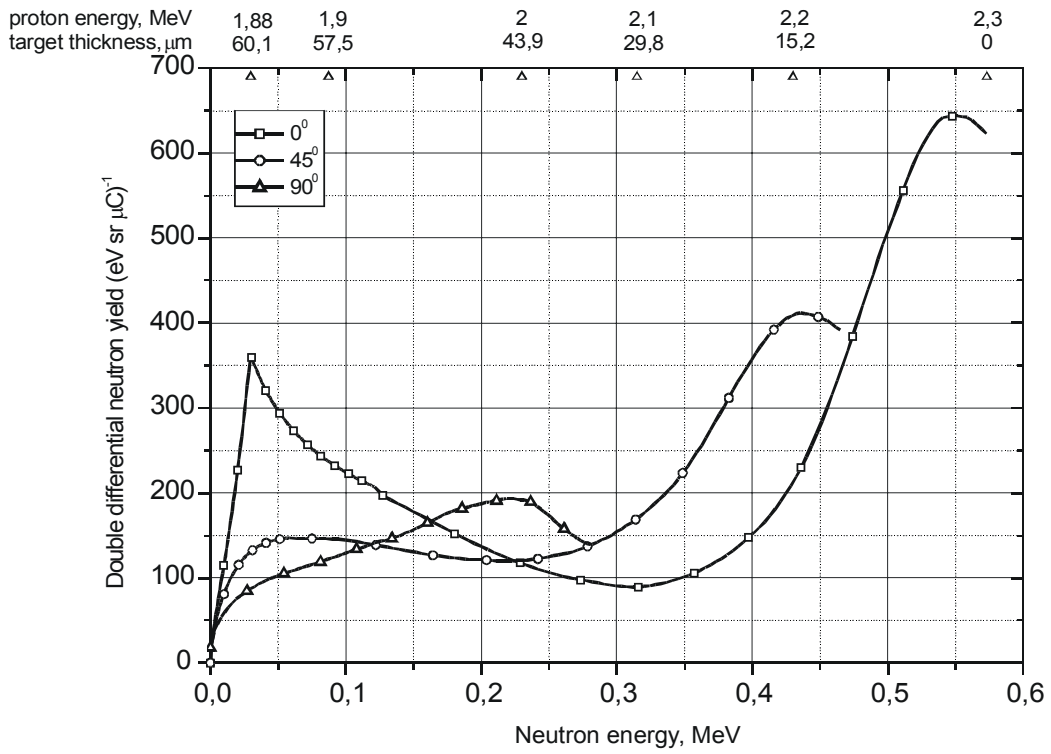
Fig. 1 Double differential neutrons yield from thick ^{7}Li target for angles 0^0, 45^0 and 90^0, initial proton energy 2.3 MeV. Top axis: proton energy and target thickness for 0^0.
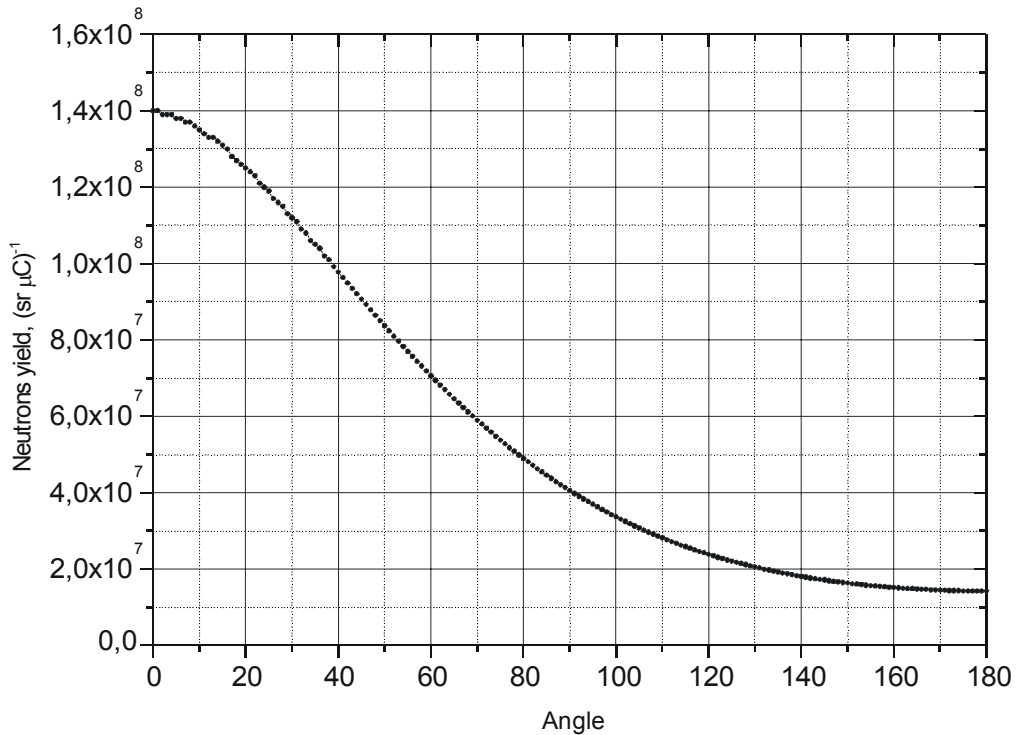
Fig. 2 Angle neutrons distribution from thick lithium target and initial proton energy 2.3 MeV.
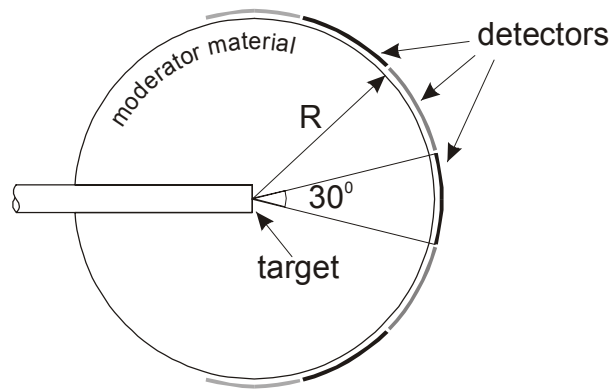
Fig. 3 Calculation model for evaluation in-air epithermal neutrons source characteristics.
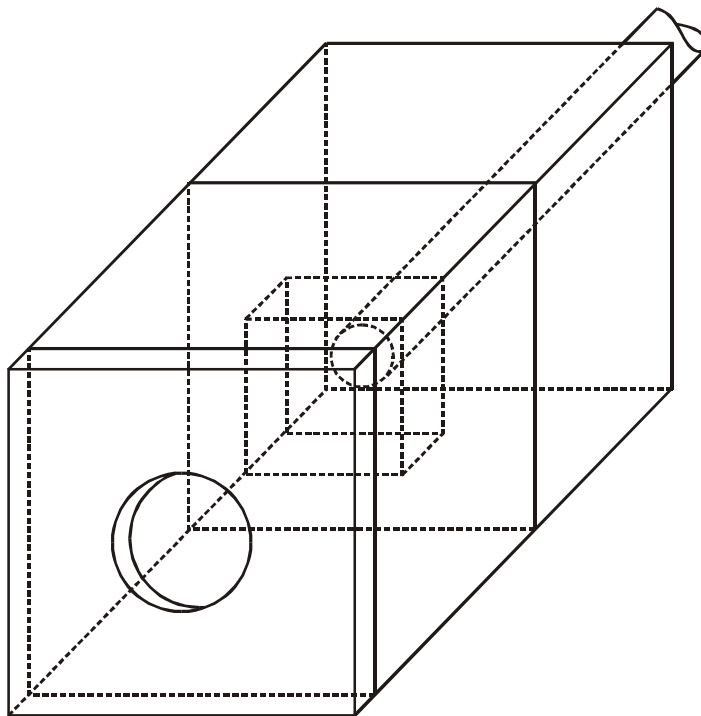
Fig. 4 Beam shaping assembly calculation model for in-phantom absorbed dose distribution modeling.
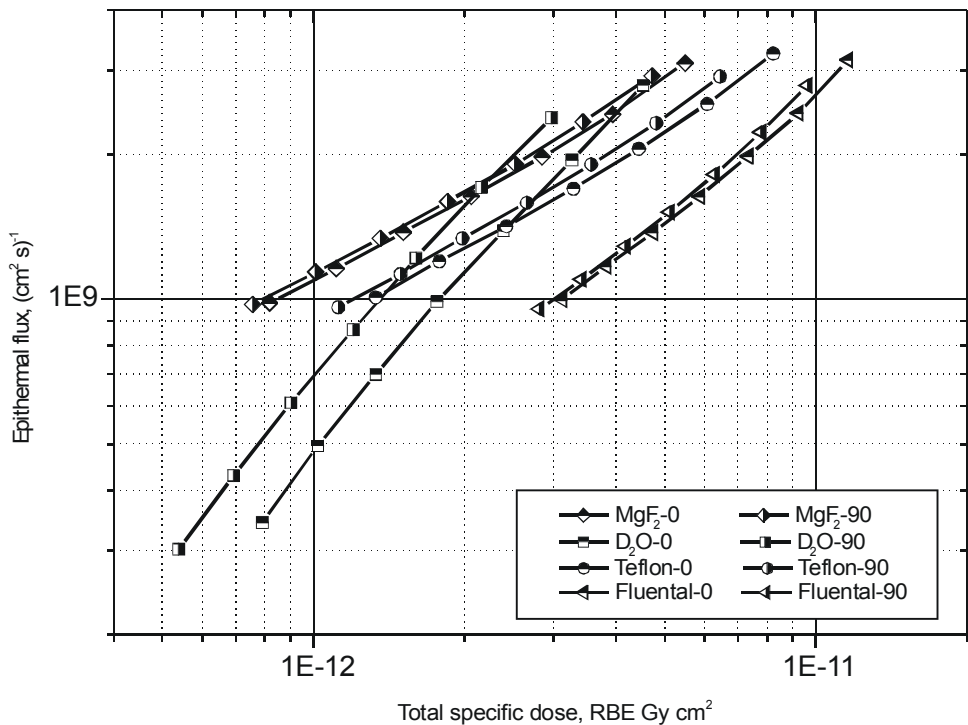
Fig 5. Epithermal neutron flux & total specific dose for various materials and moderator sizes for collinear (0^0) and orthogonal (90^0) geometry. Moderator radius from left to right 28, 26, 24, 22, 20, 18, 16 cm. For thick lithium-7 target, proton energy 2.3 MeV, proton current 10 mA.
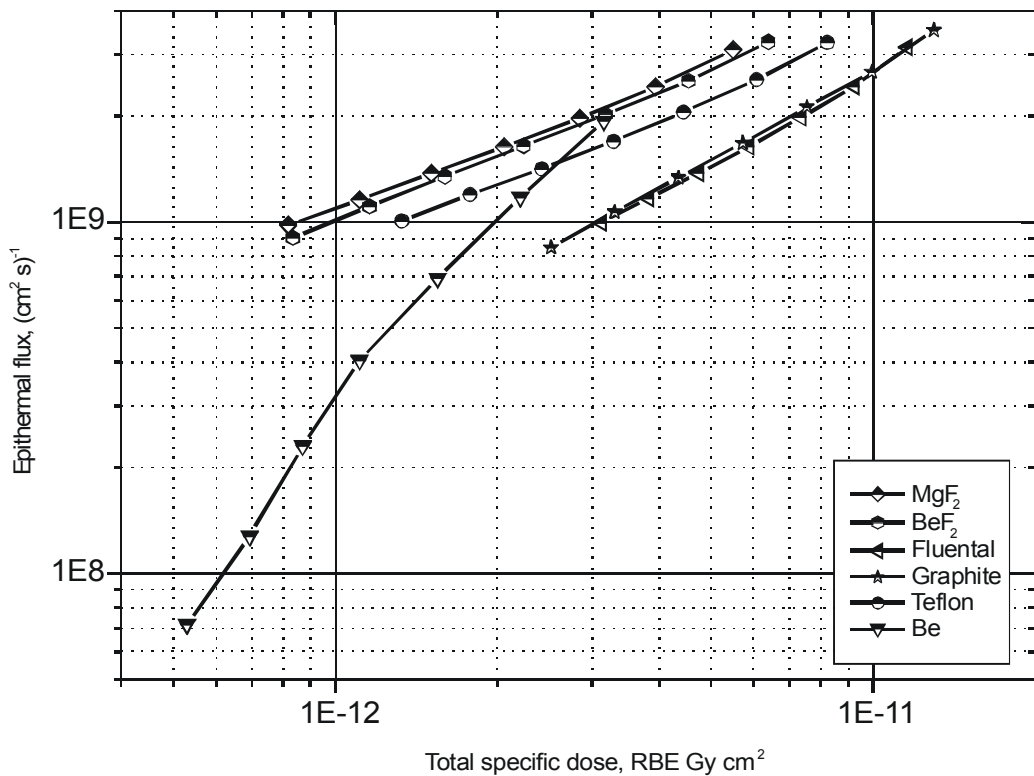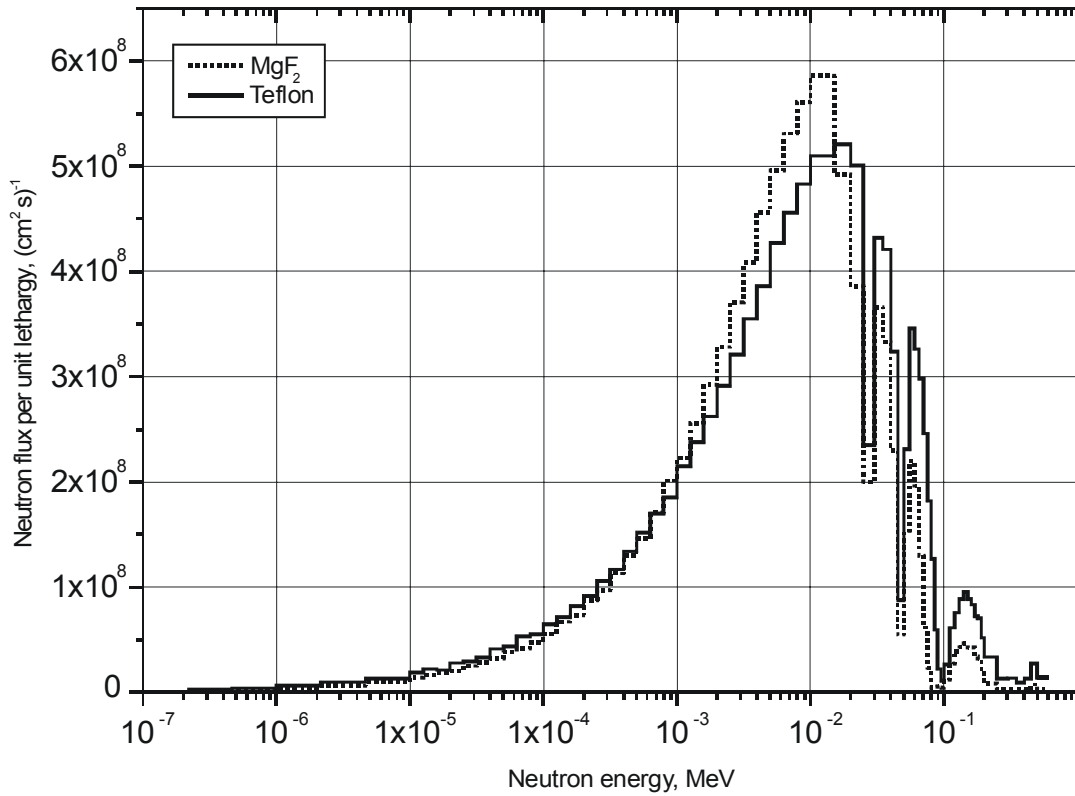

Fig 6. Epithermal neutron flux & total specific dose for various materials and moderator sizes for collinear (0^0) geometry. Moderator radius from left to right 28, 26, 24, 22, 20, 18, 16 cm. For thick lithium-7 target, proton energy 2.3 MeV, proton current 10 mA.
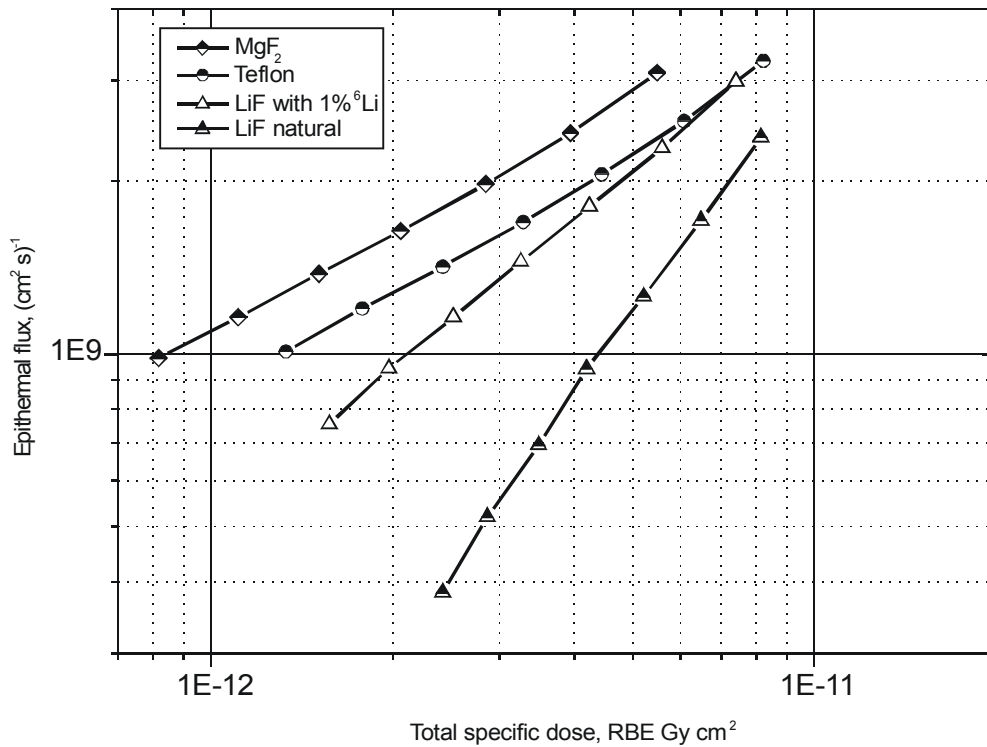
Fig 7. Epithermal neutron flux & total specific dose for MgF_2, Teflon and LiF with different ^6Li isotope concentrations for various moderator sizes, collinear (0^0) geometry. Moderator radius from left to right 28, 26, 24, 22, 20, 18, 16 cm. Thick lithium-7 target, proton energy 2.3 MeV, proton current 10 mA.
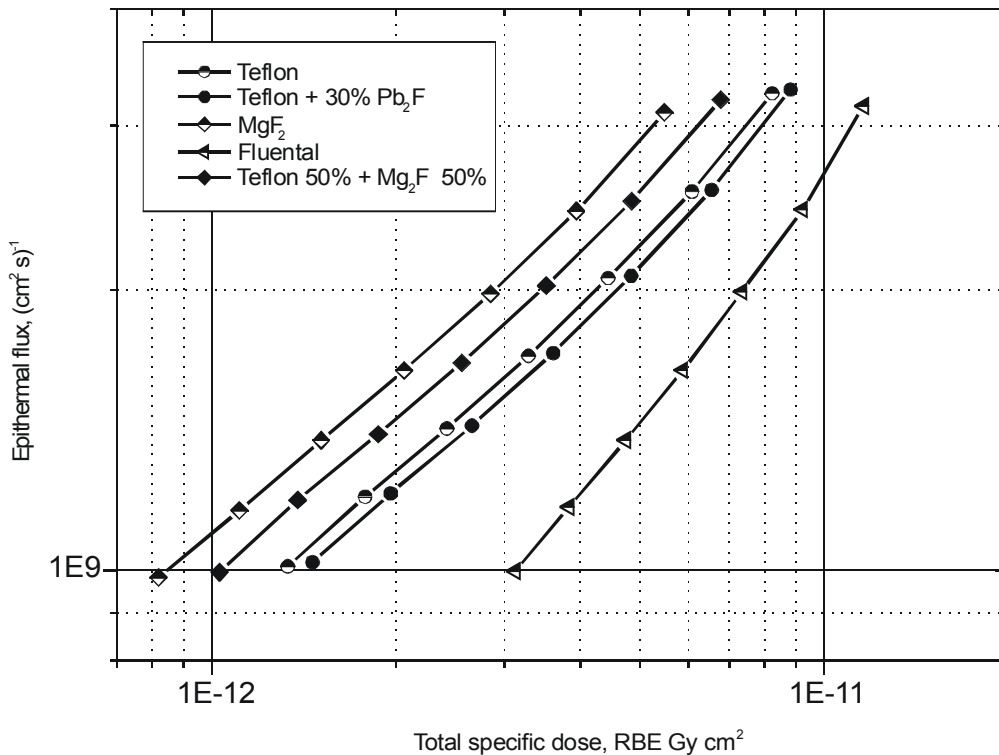

Fig 8. Epithermal neutron flux & total specific dose for MgF_2 and Teflon with different admixtures and Fluental for various moderator sizes, collinear (0^0) geometry. Moderator radius from left to right 28, 26, 24, 22, 20, 18, 16 cm. Thick lithium-7 target, proton energy 2.3 MeV, proton current 10 mA.

Fig. 9. Neutron spectra from MgF$_2$ and Teflon moderators with radius 20 cm on a proton beam direction. Proton energy 2.3 MeV, current 10 mA.
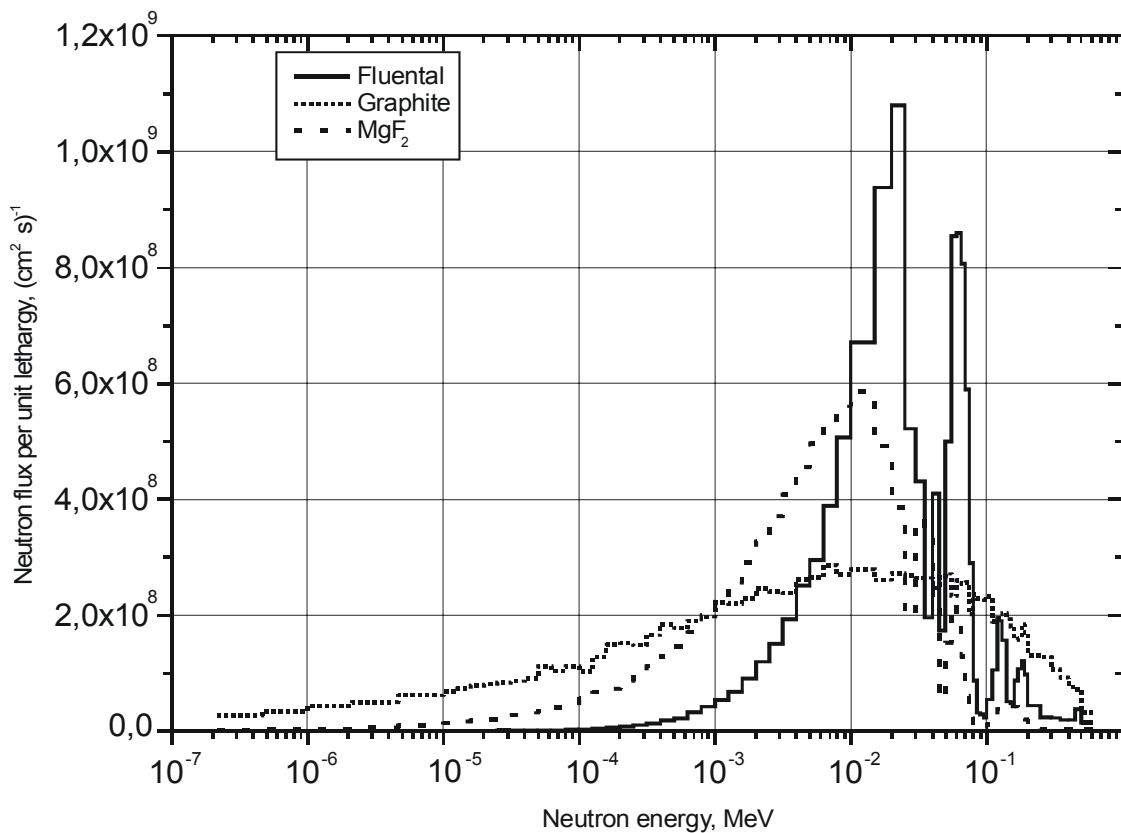
Fig. 10. Neutron spectra from Fluental, Graphite and MgF$_2$ moderators with radius 20 cm on a proton beam direction. Proton energy 2.3 MeV, current 10 mA.
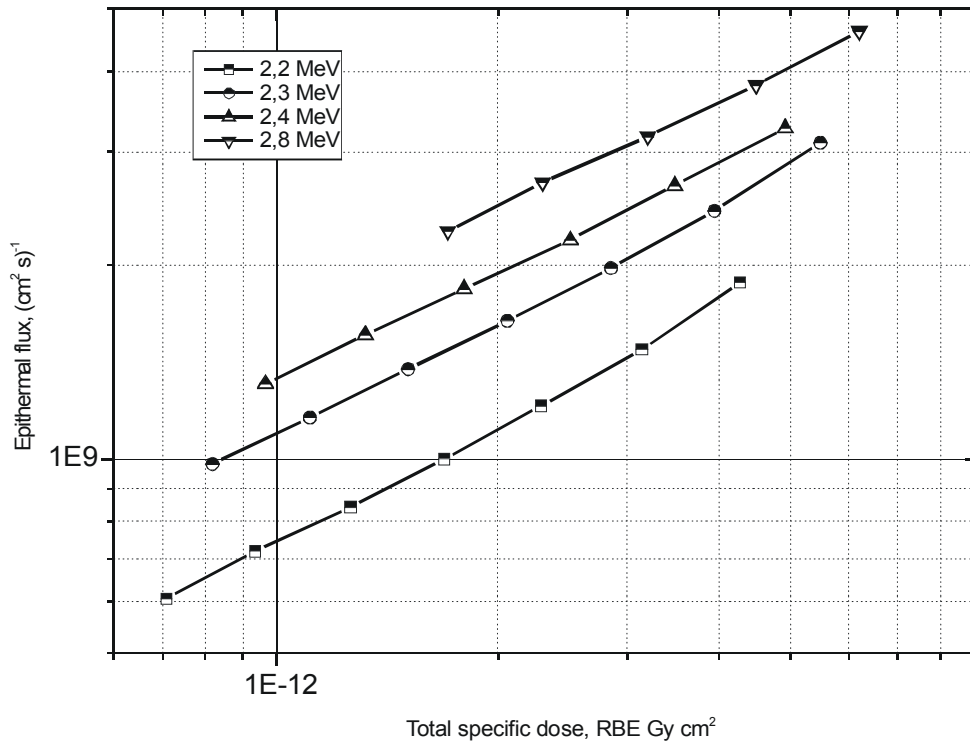
Fig 11. Epithermal neutron flux & total specific dose for MgF_2 moderator, various moderator sizes, collinear (0^0) geometry. Moderator radius from left to right 28, 26, 24, 22, 20, 18, 16 cm. Thick lithium-7 target, proton energy 2.2, 2.3, 2.4, 2.8 MeV, proton current 10 mA.
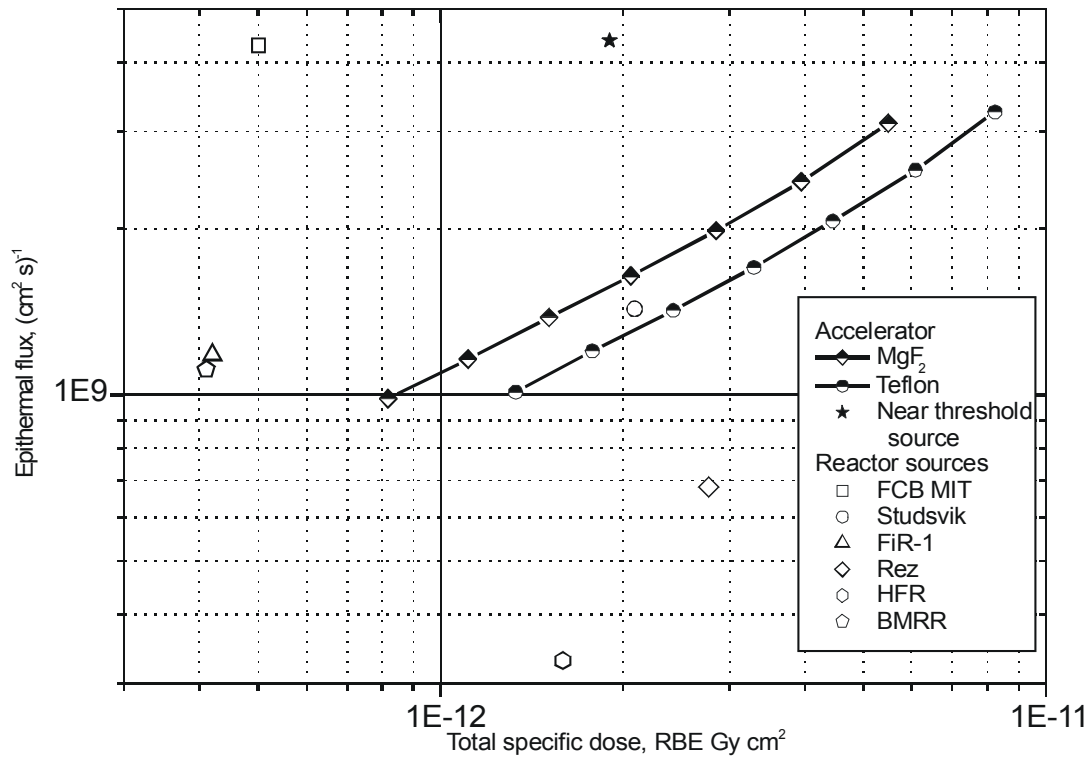
Fig. 12. Epithermal neutron sources characteristics comparison for $^7Li(p,n)^7Be$ neutron source with MgF_2 and Teflon moderators (E_p = 2,3 MeV, I_p = 10 mA),

near threshold source (E_p = 1,915 MeV, I_p = 10 mA) [19] and reactor based neutron sources [20].
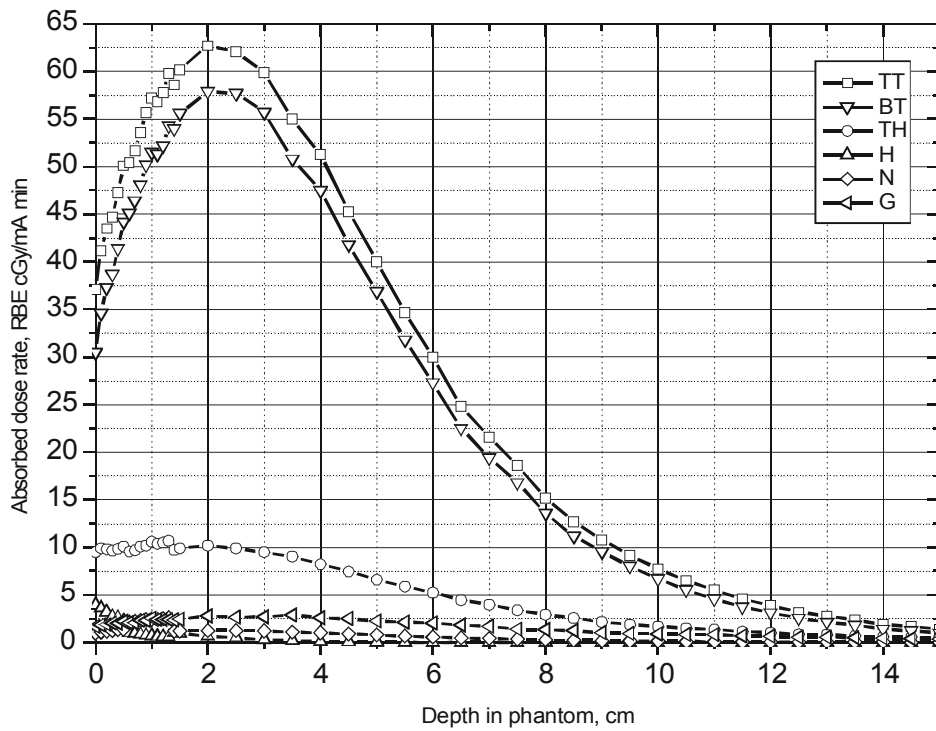
Fig. 13. Absorbed doses rates as function of depth in phantom. MgF$_2$ moderator, size 40x40x40 см, proton energy 2.3 MeV, beam current 1 mA. TT – tumor total dose, BT – boron dose in tumor, HT – total dose in healthy tissue, H – proton recoil dose, N – dose from nuclear reaction with nitrogen, G – gamma ray dose.
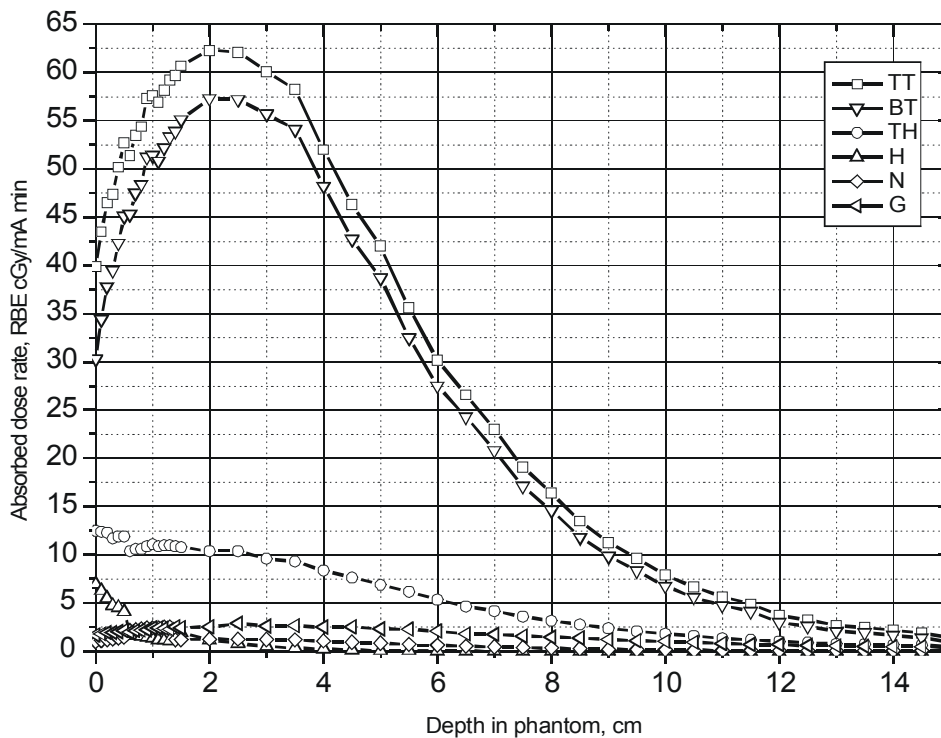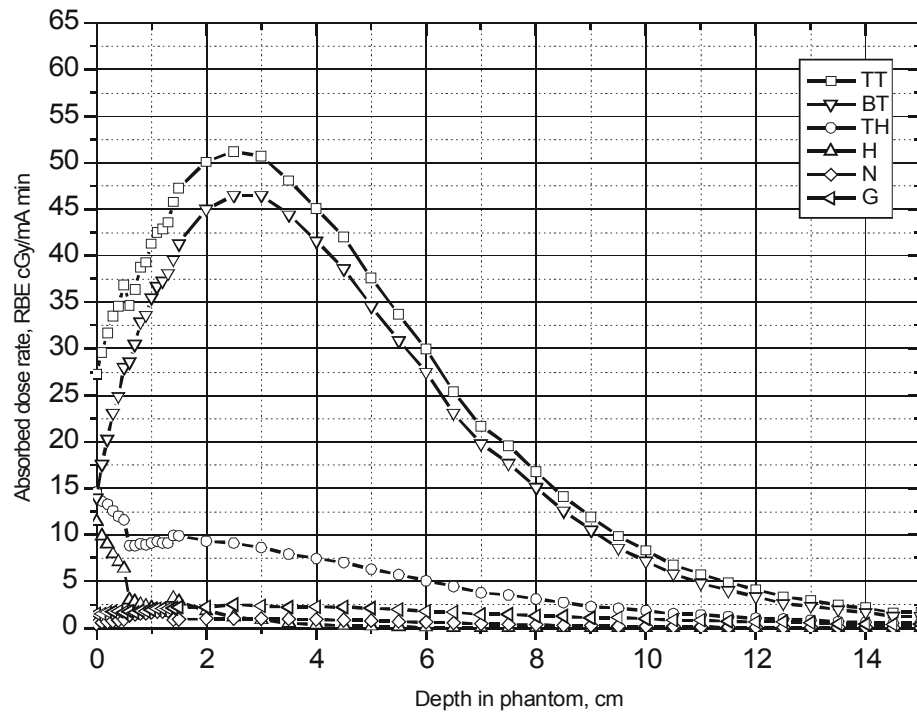

Fig. 14. Absorbed doses rates as function of depth in phantom. Polytetra-fluoroethylene moderator, size 40x40x40 см, proton energy 2.3 MeV, beam current 1 mA. TT – tumor total dose, BT – boron dose in tumor, HT – total dose in healthy

tissue, H – proton recoil dose, N – dose from nuclear reaction with nitrogen, G – gamma ray dose.
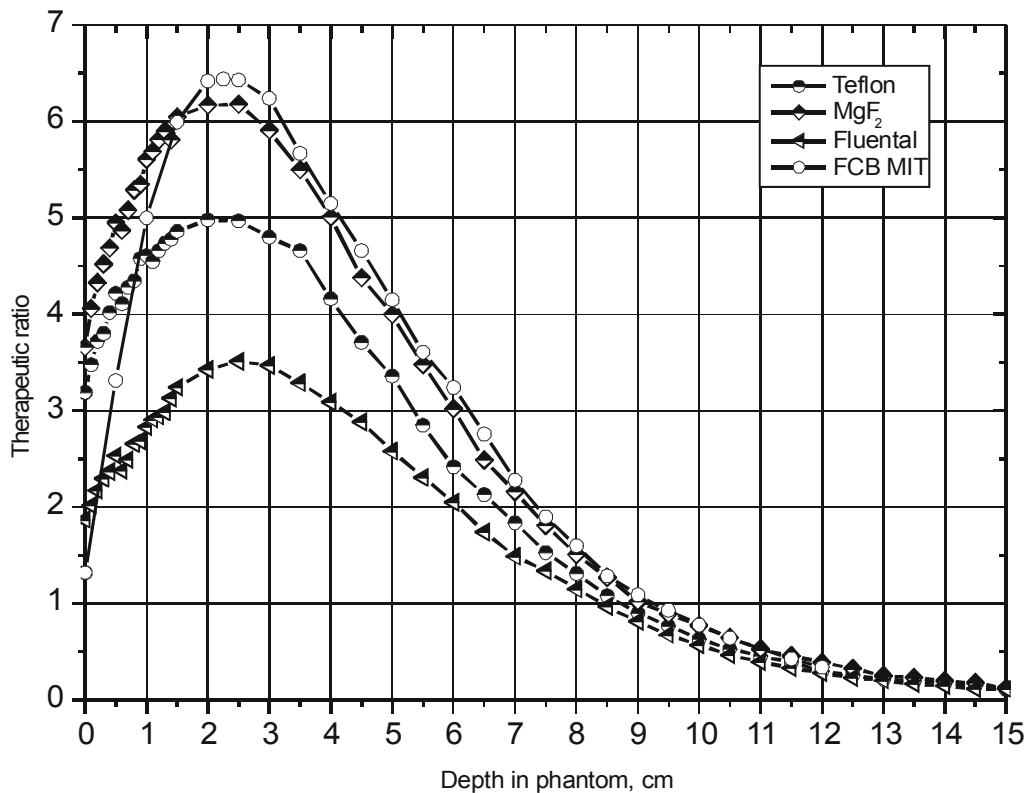

Fig. 15. Absorbed doses rates as function of depth in phantom. Fluental moderator, size 40x40x40 см, proton energy 2.3 MeV, beam current 1 mA. TT – tumor total dose, BT – boron dose in tumor, HT – total dose in healthy tissue, H – proton recoil dose, N – dose from nuclear reaction with nitrogen, G – gamma ray dose.

Fig. 16 Therapeutic ratio for different moderator materials as function of depth in phantom, moderator size 40x40x40 cm (proton energy 2.3 MeV) and reactor based beam [21].
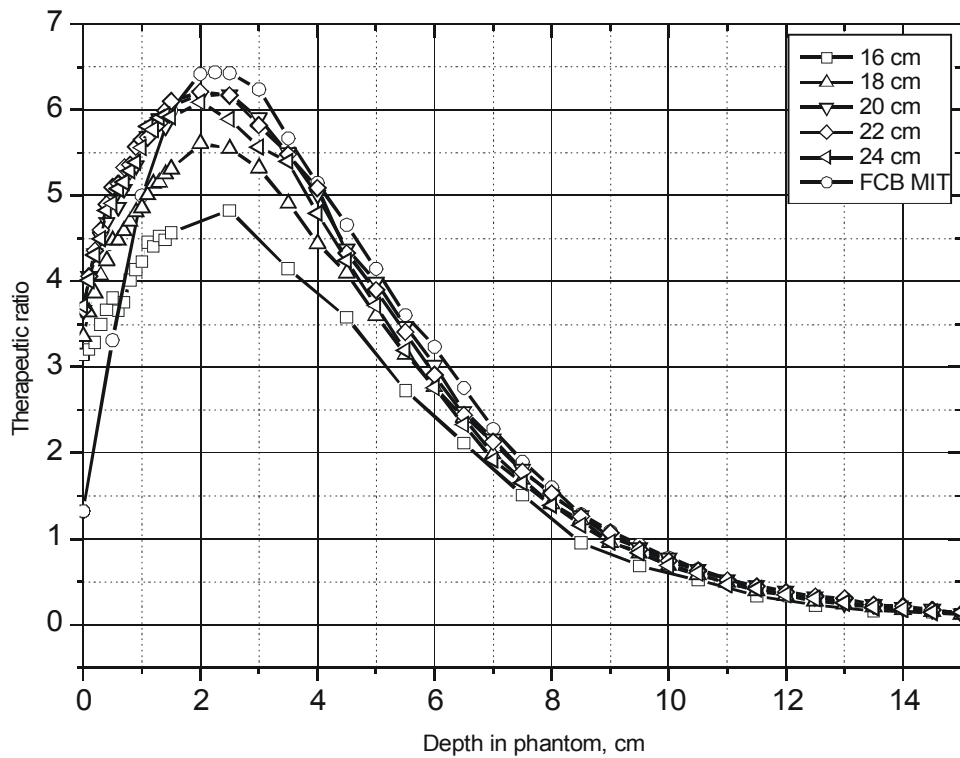
Fig. 17. Therapeutic ratio for MgF_2 – polytetrafluoroethylene moderator (size 40x40x40 cm) with various MgF_2 block length. Proton energy 2.3 MeV. FCB MIT – reactor based beam [21].
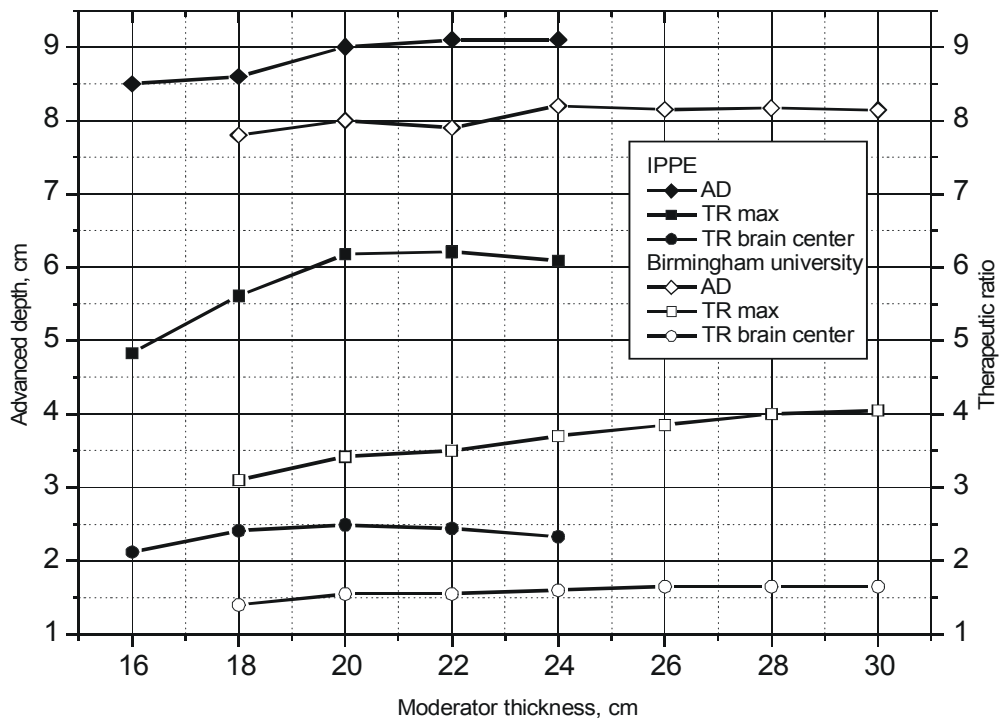

Fig. 28. Moderators characteristics comparison for MgF_2 – polytetrafluoroethylene moderator (proton energy 2.3 MeV) and Fluental and graphite reflector moderator suggested by Birmingham University team [18] (proton energy 2.4 MeV).